Available online at www.sciencedirect.com
SCIENCE DIRECT®
Journal of Magnetic Resonance 177 (2005) 93–101
JMR Journal of Magnetic Resonance
www.elsevier.com/locate/jmr

Peak suppression in ESEEM spectra of multinuclear spin systems

Stefan Stoll, Carlos Calle, George Mitrikas, Arthur Schweiger *

Physical Chemistry Laboratory, ETH Hönggerberg, 8093 Zürich, Switzerland

Received 26 May 2005; revised 30 June 2005
Available online 19 August 2005

Abstract

We have observed a disturbing suppression effect in three-pulse ESEEM and HYSCORE spectra of systems with more than one nucleus coupled to the electron spin. For such systems, the ESEEM signal contains internuclear combination peaks of varying intensity. At the same time, the peaks at the basic ESEEM frequencies are reduced in intensity, up to the point of complete cancellation. For both three-pulse ESEEM and HYSCORE, the amplitude of a peak of a given nucleus depends not only on its modulation depth parameter k and the τ-dependent blind-spot term b, but also on k and b of all other nuclei. Peaks of nuclei with shallow modulations can be strongly suppressed by nuclei with deep modulations. This cross-suppression effect explains the observation that HYSCORE ^{1}H peaks are often very weak or even undetectable in the presence of strong ^{14}N peaks. Due to this distortion of intensities, ESEEM spectra have to be analysed very carefully. We present a theoretical analysis of this effect based on the product rules, numerical computations, and illustrative experimental data on $Cu(gly)_2$. In experiments, the impact of this cross suppression can be alleviated by a proper choice of τ values, remote echo detection, and matched pulses.

Keywords: ESEEM; HYSCORE; Product rule; Cross suppression; Blind spots

1. Introduction

Three-pulse electron spin echo envelope modulation (ESEEM) and hyperfine sublevel correlation (HYSCORE) experiments are two informative pulse EPR techniques [1] often employed in the structural analysis of paramagnetic compounds containing transition metal ions [2] or organic and inorganic radicals.

These experiments have been applied extensively, and detailed information on hyperfine couplings and nuclear quadrupole interactions has been extracted from the resulting spectra, mainly based on the analysis of peak *positions*, since an accurate and general quantitative interpretation of peak *intensities* via numerical simulations has not yet been accomplished. Nevertheless, on a theoretical level, the properties of the signals generated by the two experiments have been thoroughly analysed [3–5], and destructive interference effects have been described [6].

Here we report on a suppression effect in ESEEM spectra of multinuclear systems that has passed unnoticed up to now. Nuclei with deep modulations, such as ^{14}N close to the cancellation regime, can partially or completely suppress peaks of nuclei with shallow modulations, most prominently ^{1}H and ^{19}F. This effect, which we call cross suppression, has a serious impact on spectral intensities and may lead to misinterpretation of spectral features.

The article is structured as follows. In Section 2, the basic theory of three-pulse ESEEM and HYSCORE is summarised. In Section 3, the features of three-pulse ESEEM and HYSCORE signals of systems with multiple nuclei are analysed. Section 4 presents an experimental demonstration of the suppression effect in a frozen solution of bisglycine copper(II) ($Cu(gly)_2$). Finally, the practical implications and some experimental alternatives that alleviate the impact of the suppression effect are discussed.

* Corresponding author. Fax: +41 44 632 1021.
E-mail address: schweiger@phys.chem.ethz.ch (A. Schweiger).

1090-7807/$ - see front matter © 2005 Elsevier Inc. All rights reserved.
doi:10.1016/j.jmr.2005.07.012

2. Basic theory

2.1. Model spin system

For the following discussion of suppression effects in multinuclear systems, we use a simple axially symmetric $S = 1/2$, $I = 1/2$ model system [1] with an isotropic g matrix. The nuclear frequencies are given by

$$\omega_{\alpha,\beta}/2\pi = \nu_{\alpha,\beta} = \sqrt{\left(\nu_I \pm \frac{A}{2}\right)^2 + \left(\frac{B}{2}\right)^2} \tag{1}$$

with

$$\begin{aligned} A &= T\left(3\cos^2\theta - 1\right) + a_{iso}, \\ B &= 3T\sin\theta\cos\theta. \end{aligned} \tag{2}$$

T and a_{iso} are the dipolar and the isotropic hyperfine coupling, $\nu_I = -g_n\beta_n B_0/h$ is the nuclear Larmor frequency, and θ is the angle between the electron-nuclear distance vector and the external static magnetic field vector $\boldsymbol{B}_0$. The orientation-dependent modulation depth parameter is given by

$$k(\theta) = \left(\frac{B\nu_I}{\nu_\alpha\nu_\beta}\right)^2. \tag{3}$$

It is zero at $\theta = 0°$, 90° and maximum at $\theta \approx 45°$ for small T and a_{iso}.

In the following, the quantitative discussion of the cross-suppression effect is limited to single-crystal spectra. In disordered systems, destructive interferences between signals originating from centres with similar orientations can result in an additional substantial signal suppression, as discussed in detail elsewhere [6].

2.2. Three-pulse ESEEM

For the three-pulse ESEEM experiment, π/2–τ–π/2–t–π/2–τ–echo, the time-domain signal for our model system is given by [1]

$$V_{3p}(\tau, t) = \tfrac{1}{2}\left[V^\alpha(\tau, t) + V^\beta(\tau, t)\right] \tag{4}$$

with the contribution from the α electron spin manifold

$$V^\alpha(\tau, t) = 1 - \tfrac{k}{2}\left[1 - \cos(\omega_\beta\tau)\right]\left[1 - \cos(\omega_\alpha(t + \tau))\right] \tag{5}$$

and an analogous expression for $V^\beta(\tau,t)$, obtained by interchanging α and β. τ is the constant delay between the first and the second microwave pulse, t is the variable delay between the second and the third pulse. Ideal pulses are assumed in the derivation of Eq. (4), and an overall scaling factor containing physical and experimental constants has been dropped. Using abbreviations for the amplitude

$$A_\alpha = kb_\alpha = k\frac{1 - \cos(\omega_\beta\tau)}{2} \tag{6}$$

and the oscillating part

$$c_\alpha = \cos(\omega_\alpha(t + \tau)), \tag{7}$$

V^α can be written more compactly as

$$V^\alpha = 1 - A_\alpha(1 - c_\alpha) = (1 - A_\alpha) + A_\alpha c_\alpha. \tag{8}$$

As can be seen from Eq. (6), the amplitude A_α is proportional to the modulation depth k and to a blind-spot term $b_\alpha = [1 - \cos(\omega_\beta\tau)]/2$. The amplitude of the α peak depends on the blind-spot factor containing the β nuclear frequency and vice versa. A_α lies between 0 and 1, since both k and b_α lie between 0 and 1.

The total zero-frequency component of the signal in Eq. (4) is

$$V^{(0)} = 1 - (A_\alpha + A_\beta)/2 = 1 - k(b_\alpha + b_\beta)/2. \tag{9}$$

Thus, it also depends on the k value of the nucleus: the deeper the modulations, the smaller $V^{(0)}$. In the limiting case $k = b_\alpha = b_\beta = 1$, the zero-frequency component vanishes, and the echo amplitude oscillates around zero. For disordered systems with broad ESEEM lines, where the nuclear coherences (NCs) dephase during the dead time of the spectrometer, the suppression of $V^{(0)}$ may lead to an almost complete cancellation of the echo. Thus, even under favourable relaxation conditions, a weak three-pulse echo does not necessarily indicate a low concentration of the paramagnetic species.

2.3. HYSCORE

The time-domain signal resulting from a HYSCORE experiment, π/2–τ–π/2–t_1–π–t_2–π/2–τ–echo, is given by

$$V_{4p}(\tau, t_1, t_2) = \tfrac{1}{2}[V^{\alpha\beta}(\tau, t_1, t_2) + V^{\beta\alpha}(\tau, t_1, t_2)], \tag{10}$$

where $V^{\alpha\beta}$ consists of a constant offset term and terms describing the correlation peaks at $(\pm\nu_\alpha, 0)$, $(0, \pm\nu_\beta)$ and $(\pm\nu_\alpha, \pm\nu_\beta)$ in frequency domain. The second term in Eq. (10), $V^{\beta\alpha}$, describes an analogous set of peaks. Hence, there are two cross peaks in each quadrant of the two-dimensional (2D) spectrum. All other contributions are usually removed by baseline corrections. However, for a correct description of systems with more than one nucleus, these terms must be included.

The intensity of a cross peak at $(\pm\nu_\alpha, \pm\nu_\beta)$ is given by

$$A_{\alpha\beta} = kz^2 b_{\alpha\beta} = kz^2 \sin\frac{\omega_\alpha\tau}{2}\sin\frac{\omega_\beta\tau}{2}. \tag{11}$$

For peaks in the (+,+) quadrant

$$z^2 = c^2 = \frac{\left|\nu_I^2 - (\nu_\alpha - \nu_\beta)^2\right|}{\nu_\alpha\nu_\beta}, \tag{12}$$

and in the (−,+) quadrant

$$z^2 = 1 - c^2. \tag{13}$$

In Eq. (11), kz^2 describes the contribution resulting from different mixing of the nuclear Zeeman states in the α and β electron spin manifolds, whereas $b_{\alpha\beta}$ de-

scribes a τ-dependent factor that gives rise to blind spots at $\nu_{\alpha,\beta} = n/\tau$. In disordered systems, additional amplitude effects due to destructive interferences have to be taken into account [6].

3. Multinuclear systems

3.1. Three-pulse ESEEM

For a system with N nuclei with spin $I = 1/2$ coupled to an $S = 1/2$ electron spin, the three-pulse ESEEM signal can be written as the product [7]

$$V_{3p}(\tau,t) = \frac{1}{2}\left[\prod_{q=1}^{N} V_q^{\alpha}(\tau,t) + \prod_{q=1}^{N} V_q^{\beta}(\tau,t)\right], \tag{14}$$

where V_q^{α} and V_q^{β} are the signals that would be obtained if only nucleus q was coupled to the electron spin.

This product rule is only valid when ideal pulses are assumed. Ideal pulses have zero duration and thus have infinite bandwidth. In addition, they are assumed to be infinitely strong, so that the static Hamiltonian is negligible during the pulse. Although the latter approximation is valid for strong pulses, their bandwidth is not infinite. The shortest $\pi/2$ pulses commonly employed have a length of about 8 ns and a centre-lobe FWHH bandwidth of about 100 MHz. In addition, the bandwidth of X-band resonators in pulse EPR rarely exceeds 100 MHz. Hence, NCs with frequencies larger than 100 MHz are only partially detectable, if at all. If this limited bandwidth is taken into account adequately, numerical simulations show that the product rule is a reasonably good approximation for pulses with a length up to 16 ns.

Since Eq. (14) is the sum of two products in time domain, in frequency domain it corresponds to the sum of a convolution of all α spectra and a convolution of all β spectra. Thus, in systems with two nuclei with $I = 1/2$, in addition to single-quantum (SQ) peaks at $\nu_{\alpha 1}$ and $\nu_{\alpha 2}$, combination peaks between nuclear frequencies within the same electron spin manifold (α or β) appear, with frequencies

$$\nu_{\alpha\pm} = \nu_{\alpha 1} \pm \nu_{\alpha 2}, \qquad \nu_{\beta\pm} = \nu_{\beta 1} \pm \nu_{\beta 2}. \tag{15}$$

The sums correspond to double-quantum (DQ) transitions, and the differences correspond to zero-quantum (ZQ) transitions. There are no combination frequencies of the form $\nu_{\alpha 1} \pm \nu_{\beta 2}$, since there are no NCs with such frequencies that could evolve during time t. Only electron coherences can contain nuclear frequencies from different electron spin manifolds.

The fact that the product rule leads to combination peaks is generally known [8]. However, the effect of the product rule on peak *intensities* has not yet been fully appreciated. It can have severe experimental consequences, causing a possibly complete suppression of SQ peaks of nuclei with small k values in systems which additionally contain nuclei with large k values.

As in Section 2.2, we discuss the signal due to NCs in the α manifold only. The NCs in the β manifold can be obtained by exchanging α and β in all the expressions. By combining Eq. (14) (dropping the pre-factor 1/2) and Eq. (8) we get for the amplitude of the zero-frequency component

$$\prod_q (1 - A_{\alpha q}) + \prod_q (1 - A_{\beta q}), \tag{16}$$

for the SQ peaks at $\nu_{\alpha q_1}$

$$A_{\alpha q_1} \prod_{q \neq q_1} (1 - A_{\alpha q}), \tag{17}$$

and for the DQ and ZQ peaks at $\nu_{\alpha q_1} \pm \nu_{\alpha q_2}$

$$\frac{1}{2} A_{\alpha q_1} A_{\alpha q_2} \prod_{q \neq q_1, q_2} (1 - A_{\alpha q}). \tag{18}$$

Similar terms are obtained for higher multiple-quantum (MQ) peaks with frequencies $\nu_{\alpha q_1} \pm \nu_{\alpha q_2} \pm \ldots$. Obviously, for each additional nucleus q, the α-SQ peak amplitude of nucleus q_1 is reduced by a factor of $(1 - A_{\alpha q})$. The larger the amplitudes $A_{\alpha q}$, the stronger is the suppression effect on the amplitude of nucleus q_1.

In the simplest case of two nuclei, the α term in Eq. (14) becomes

$$\begin{aligned} V_1^{\alpha} V_2^{\alpha} = {} & (2 - A_{\alpha 1} - A_{\alpha 2} + D_{\alpha}) + (A_{\alpha 1} - D_{\alpha}) c_{\alpha 1} \\ & + (A_{\alpha 2} - D_{\alpha}) c_{\alpha 2} + D_{\alpha} c_{\alpha 1} c_{\alpha 2}, \end{aligned} \tag{19}$$

where

$$\begin{aligned} D_{\alpha} &= A_{\alpha 1} A_{\alpha 2} = k_1 k_2 b_1 b_2 \\ &= k_1 k_2 \frac{[1 - \cos(\omega_{\beta 1}\tau)]}{2} \frac{[1 - \cos(\omega_{\beta 2}\tau)]}{2}, \end{aligned} \tag{20}$$

with $0 \leqslant D_{\alpha} \leqslant 1$. The amplitudes of the SQ peaks are *reduced* by D_{α}, whereas the zero-frequency component is *increased* by D_{α}. The ZQ and DQ peak amplitudes are increased by $D_{\alpha}/2$. In total, the sum of the intensities of all peaks is conserved. The effect on the peak intensities is illustrated in Fig. 1. In the case of a maximum modulation depth for nucleus 1, i.e., $A_{\alpha 1} = 1$, the peak at $\nu_{\alpha 2}$ is *completely* suppressed.

According to Eq. (6) and Eq. (17), the suppression of an α-SQ peak depends both on k and on the blind-spot term b_{α} (containing the β-SQ frequencies) of all the other nuclei. Thus, for spin systems with several nuclei, the blind-spot behaviour becomes much more complicated.

In a three-pulse ESEEM experiment, the only way to control the peak amplitudes is via the inter-pulse distance τ. The $\alpha(\beta)$ peak of nucleus 2 will be best visible if it is not suppressed by the τ-dependent factor b and if the $\beta(\alpha)$ peak of nucleus 1 is suppressed.

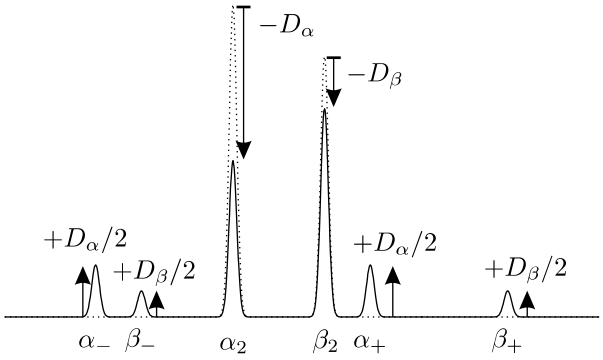

Fig. 1. Schematic representation of the cross-suppression effect in three-pulse ESEEM experiments: a nucleus 1 with deep modulations affects the peak amplitudes of nucleus 2. The zero-frequency component and the SQ peaks of nucleus 1 are not shown. Dotted, nucleus 1 is absent; solid, nucleus 1 is present.

For two magnetically equivalent $I = 1/2$ nuclei, the coincident α-SQ peaks have a total amplitude of $2A_\alpha(1 - A_\alpha)$, which is maximum at $A_\alpha = 1/2$ and zero for $A_\alpha = 1$. Consequently, in the case of a deep modulation ($k \approx 1$) and no reduction of the β frequency due to the τ-dependent term ($b_\alpha \approx 1$), the α peak is completely suppressed. The amplitude of the ZQ and DQ peaks is then given by $A_\alpha^2/2$, which is maximum at $A_\alpha = 1$.

The analysis given above is valid for single crystals. For disordered systems, orientational distributions have to be taken into account. Many of the ZQ and DQ peaks are broad and are reduced in intensity due to their rapid dephasing during the dead time. Additionally, k_1 and k_2 depend on the orientation of $\boldsymbol{B}_0$ (see Eq. (3)), so the suppression effect will also depend on the $\boldsymbol{B}_0$ orientation and on the relative orientation between the hyperfine tensors. This is illustrated in Fig. 2, which shows the effect of a ^{13}C nucleus with deep modulations on the SQ peaks of a proton. Depending on τ, one or both ^{1}H-SQ peaks are partially suppressed by the ^{13}C nucleus. For $\tau \approx 100$ ns, a commonly used region, the suppression is almost complete. For larger τ values, additional blind spots are introduced.

Qualitatively, the conclusions made above can be extended to two-pulse ESEEM [1], where the product rule [8] has the simple form

$$V_{2p}(\tau) = \prod_{q=1}^{N} V_q(\tau). \tag{21}$$

Due to the presence of peaks at frequencies $\nu_{\alpha q} \pm \nu_{\beta q}$, the signal cannot be decomposed into α and β contributions. The spectrum of a multinuclear system results from the convolution of the spectra of all one-nucleus subsystems.

3.2. Matrix protons

Potentially, the presence of a large number of matrix protons could have a suppressing effect on the intensity of other more strongly coupled nuclei, such as a proton closer to a paramagnetic centre. This has been studied using Eq. (5) and the product rule Eq. (14). If present, the effect should be largest for water, the solvent with the highest ^{1}H density. As a reasonable model for the matrix, a force-field optimised spherical cluster of water molecules having a density close to the one of liquid water was used.

In our simulations, the matrix line is due to the approx. 60,000 protons located between 600 pm and

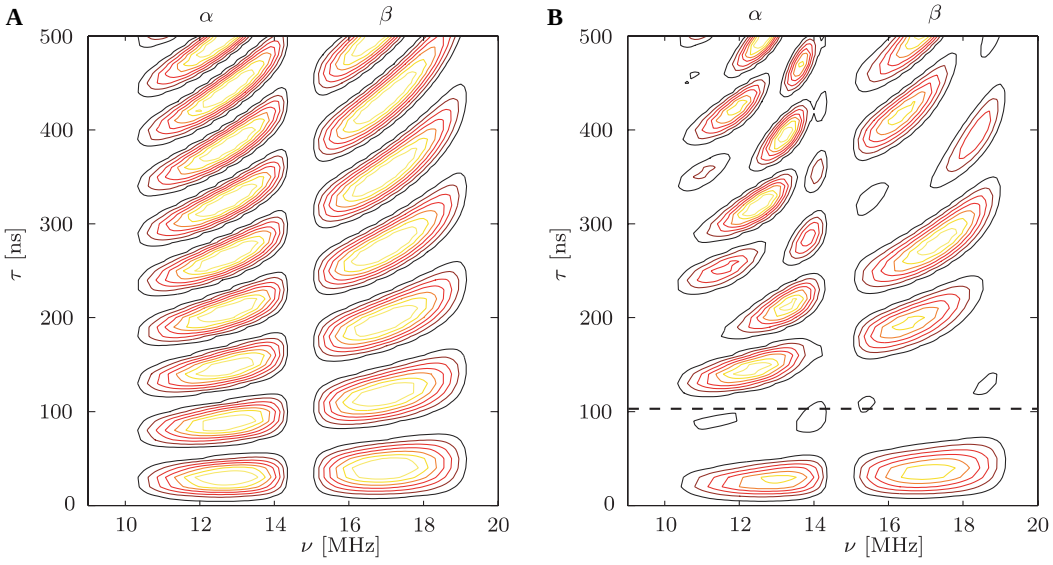

Fig. 2. Simulated τ dependence of α- and β-SQ peak intensities of a proton in a three-pulse ESEEM powder spectrum of a ^{13}C and ^{1}H nuclear spin system, using Eq. (14). Spin Hamiltonian parameters are listed in Table 1 (nuclei A and B). (A) Proton only, showing the usual blind-spot behaviour, (B) an additional ^{13}C is present, leading to cross-suppression effects. $B_0 = 345$ mT. Dashed line: almost complete ^{13}C–^{1}H cross suppression.

6 nm from the electron spin (T between 350 and 0.37 kHz). Protons with a distance of more than 6 nm from the electron spin do not affect the intensity of the matrix peak due to the very small modulation depths.

We have found that such a matrix line reduces the intensity of more strongly coupled protons by at most 10%, depending on the orientation of the closest matrix protons and the τ value. The suppression effect is strongest for $\tau \approx n/\nu_{1H}$. For all practical purposes, the influence of a matrix peak on the intensity of other lines can be neglected. On the other hand, a nucleus with deep modulations will have a pronounced effect on the matrix line.

3.3. HYSCORE

The product rule for HYSCORE [9]

$$V_{4p}(\tau,t_1,t_2) = \frac{1}{2}\left[\prod_{q=1}^{N} V_q^{\alpha\beta}(\tau,t_1,t_2) + \prod_{q=1}^{N} V_q^{\beta\alpha}(\tau,t_1,t_2)\right] \tag{22}$$

is similar to Eq. (14). $V_q^{\alpha\beta}$ is the signal from nucleus q correlating the NC with frequency $\nu_{\alpha q}$ evolving during the first evolution period t_1 with the NC with frequency $\nu_{\beta q}$ evolving during the second evolution period t_2. The explicit analytical expressions for $V_q^{\alpha\beta}$ and $V_q^{\beta\alpha}$ for $N = 2$ are lengthy, and an analysis analogous to three-pulse ESEEM does not give much new physical insight.

In frequency domain, the product rule Eq. (22) describes separate two-dimensional convolutions of the $\alpha\beta$ and the $\beta\alpha$ subspectra. For the total $\alpha\beta$ spectrum, this means that several new cross peaks involving dinuclear MQ coherences $\nu_{\alpha\pm}$ and $\nu_{\beta\pm}$ (cf. Eq. (15)) will appear. Due to the fact that such coherences occur only between nuclear sublevels in the same electron spin manifold and that cross peaks in HYSCORE can only be observed between coherences of different electron spin manifolds, *relative signs* of hyperfine couplings can be obtained from an analysis of the positions of MQ cross peaks (see, e.g. [10]). The same applies to the 2D three-pulse ESEEM experiment [1].

The blind spot behaviour of SQ/SQ cross peaks is given by $b_{\alpha\beta}$ in Eq. (11). Due to the product formula Eq. (22), the blind-spot behaviour is significantly more complicated for cross peaks involving MQ coherences.

For two nuclei with $I = 1/2$ there are four NCs in each electron spin manifold, the SQ coherences $\nu_{\alpha 1}$ and $\nu_{\alpha 2}$, the DQ coherence $\nu_{\alpha+}$ and the ZQ coherence $\nu_{\alpha-}$ and a similar set in the β manifold. Consequently, there are 32 cross peaks in each quadrant, 16 $\alpha\beta$ and 16 $\beta\alpha$ cross peaks [11], as can be seen in Fig. 3. Similar to the three-pulse ESEEM experiment, MQ/SQ and MQ/MQ peaks appear at the expense of the SQ/SQ peaks. Again, the sum of all intensities (including all terms in Eq. (10)) is conserved. The large number of cross peaks both in the (+,+) and the (−,+) quadrant contain redundant information and severely affect the intensities of the SQ/SQ peaks. In practical situations, the intensity of many cross peaks can fall below the noise level, even if the SQ/SQ cross peaks would be detectable in the absence of nuclei with deep modulations.

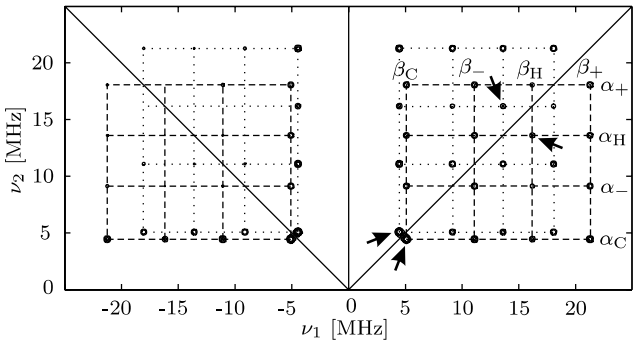

Fig. 3. Numerical simulation of a single-crystal HYSCORE spectrum, $\theta = 57°$, $B_0 = 345$ mT, all pulse lengths 16 ns, $\tau = 120$ ns. Data from Table 1 (nuclei A and B). Dashed, $\alpha\beta$ cross peaks; dotted, $\beta\alpha$ cross peaks. Arrows, SQ/SQ correlation peaks.

The situation is even worse in HYSCORE spectra of disordered systems, where the excitation of only a limited orientational range, peak broadenings due to the remaining orientational distribution, and signal suppressions due to orientational phase interference [6] lead to a further reduction of the overall intensity. Fig. 4 illustrates these effects with two exemplary simulations of powder HYSCORE spectra. In Fig. 4A, the spectrum of a system containing a proton (weak coupling case, $|A| < 2|\nu_I|$) and a ^{13}C nucleus with small hyperfine coupling and a shallow modulation depth (see Table 1, nuclei A and C) is shown. In Fig. 4B, the ^{13}C hyperfine coupling constant is increased by a factor of 10 leading to a modulation depth close to 1 (Table 1, nuclei A and B). In Fig. 4A, the ^{1}H SQ/SQ peaks dominate the spectrum. Cross peaks containing ZQ and DQ coherences are very weak. The presence of the ^{13}C nucleus with deep modulations in Fig. 4B causes intense ^{13}C-SQ/SQ peaks around 5 MHz and results in the appearance of many MQ/MQ and MQ/SQ cross ridges, distributed over both quadrants. This strongly reduces the intensity of the ^{1}H-SQ/SQ peaks (indicated by arrows).

Whether the MQ cross ridges appear in the (+,+) or the (−,+) quadrant depends on their angle of inclination with respect to the frequency axes [6]. In our example, cross peaks containing the ^{13}C-SQ frequency of the α manifold and the ZQ frequency of the β manifold (connected by a dashed line in Fig. 4B) appear in the (−,+) quadrant, which usually features peaks only in the strong coupling case $|A| > 2|\nu_I|$. The inter-pair distance of 7 MHz $\approx 2|\nu_{^{13}C}|$ could potentially lead to the wrong conclusion that a strongly coupled ^{13}C is present.

In disordered systems, the cross suppression varies with orientation via $k(\theta)$. The effect can be very strong for a small range of orientations, thus giving rise to

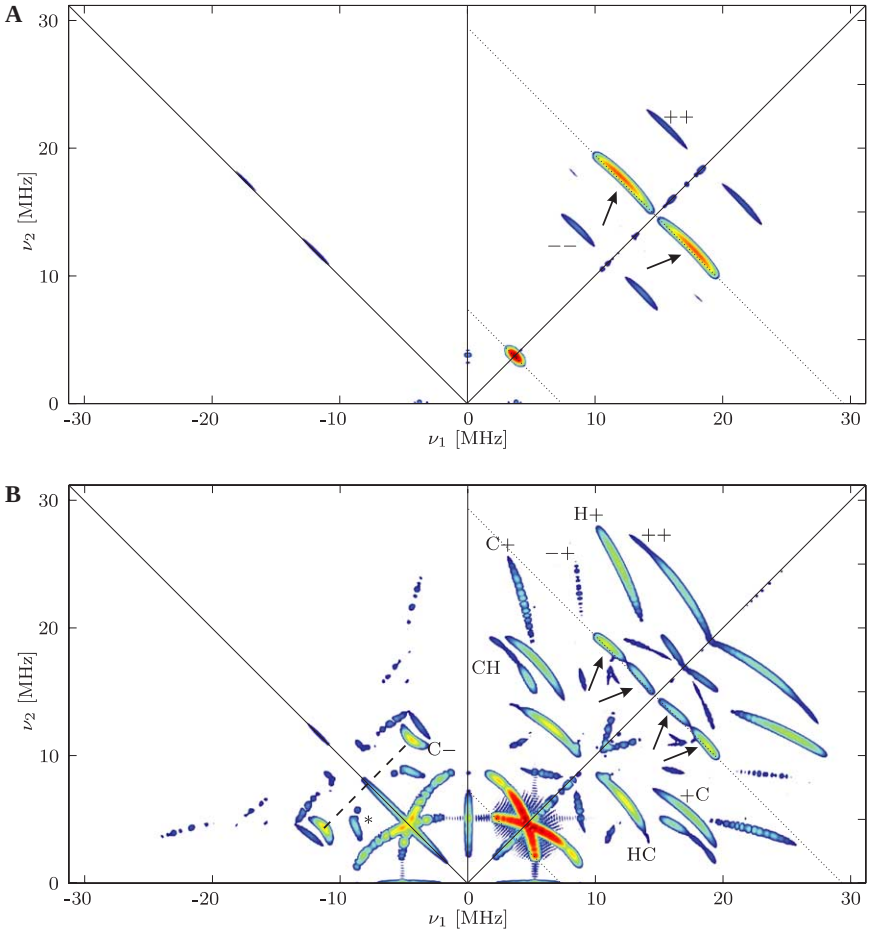

Fig. 4. Simulations of powder HYSCORE spectra (data from Table 1). (A) Nuclei A (^{1}H) and C (^{13}C with small hyperfine coupling), (B) nuclei A (^{1}H), and B (^{13}C with larger hyperfine coupling). $B_0 = 345$ mT, $\nu_{mw} = 9.6574$ GHz, $\tau = 120$ ns, all pulse lengths 16 ns. Only $\alpha\beta$ correlations are labelled in a shorthand notation, where +C means $(\nu_{\alpha+}, \nu_{\beta C})$, −+ indicates $(\nu_{\alpha-}\nu_{\beta+})$, etc. The cross peak ∗ in the (−,+) quadrant is a $(\nu_{\beta\_}, \nu_{\beta C})$ correlation due to the finite length of the π pulse. Intensities are shown on a logarithmic scale. Arrows indicate the ^{1}H SQ/SQ peaks.

Table 1
Nuclear parameters used in the simulations

Nucleus	a_{iso} (MHz)	T (MHz)	ν_I (MHz)	k_{max}
A: ^{1}H	3.0	3.5	14.7	0.126
B: ^{13}C	1.3	4.4	3.7	0.999
C: ^{13}C	0.13	0.44	3.7	0.032

suppressed regions that divide a ridge into two parts. This is visible in the ^{1}H-SQ/SQ ridges in Fig. 4B (marked by arrows).

4. Experiments

A clean experimental isolation of the cross-suppression effect is only possible via a comparison of two isotope-substituted samples, where the first one contains a nucleus with $I \geqslant 1/2$ and deep modulation, and the second contains an isotope of the same element with $I = 0$. This way, the effect of this nucleus on another nucleus with weak modulation, present in both isotopomers, could be isolated.

Unfortunately, in systems that suffer most from the cross-suppression effect, such as transition metal complexes with deep ^{14}N modulations, a substitution with the only other stable nitrogen isotope ^{15}N does not substantially reduce the amplitudes of the nitrogen peaks, unless the hyperfine coupling is almost isotropic.

A common element where a clean comparison is possible, is carbon. ^{13}C has a nuclear spin 1/2, whereas ^{12}C has no nuclear spin. Unfortunately, in most systems ^{13}C nuclei have small k values. Nevertheless, as an illustrative example for the effects arising in ESEEM spectra of multinuclear systems, two frozen degassed solutions of $Cu(gly)_2$ in 1:1 water/glycerol were measured: Sample A contained glycine with ^{13}C in natural abundance (1.1%), whereas in sample B fully ^{13}C-labelled glycine was used. The samples were of equal volume and equal concentration. The amounts of Cu^{2+} ions in the two samples as determined from cw EPR spec-

tra were equal to within 0.8%. This way the effect of ^{13}C spins on the ^{1}H ESEEM signals can be demonstrated.

X-band three-pulse ESEEM and HYSCORE spectra of samples A and B were measured at 15 K on a Bruker ELEXSYS E580 spectrometer. For three-pulse ESEEM, the magnetic field was set to 280 mT at the low-field end of the frozen-solution spectrum, corresponding to a single-crystal like orientational distribution with the magnetic field perpendicular to the molecular plane defined by the two glycine ligands [12]. All three $\pi/2$ pulses had a length of 16 ns, and the signal was detected by integrating the stimulated echo over a 24 ns window centred around the echo maximum. The usual four-step phase cycle [1] was used to remove echo crossings.

Since the two isotopomeric complexes have identical chemical structure and the two samples contain the same number of spins and all experimental settings were identical, echo amplitudes are directly comparable without any scaling or normalisation. The time-domain signals for two different τ values are shown in Fig.5, the corresponding spectra in Fig.6.

The effect of τ on the zero-frequency component as predicted by Eq. (8) is clearly visible in Fig.5 (indicated by arrows). For $\tau = 180$ ns (Fig. 5A and Fig.6A), the blind-spot term b (see Eq. (6)) suppresses the ^{13}C region in sample B (red), so that the presence of ^{13}C does not significantly lower the amplitude of the zero-frequency component. The initial overall echo amplitudes are almost identical. For $\tau = 420$ ns (Fig. 5B and Fig.6B), the situation is different. The ^{13}C peaks have appreciable intensity, and the zero-frequency component is reduced by a factor of 2. Additionally, the overall echo amplitudes at $t = 0$ are very different. This is due to the fact

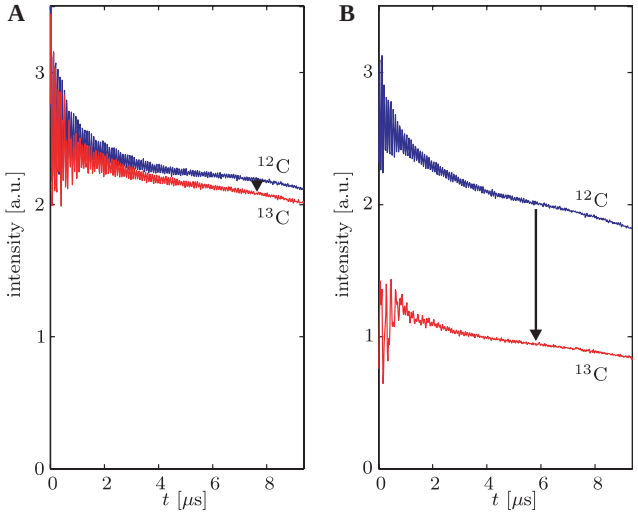

Fig. 5. Three-pulse ESEEM time-domain signals of $Cu(gly)_2$ with carbon in natural abundance (blue) and ^{13}C-labelled glycine (red) for (A) $\tau = 180$ ns and (B) $\tau = 420$ ns. (For interpretation of the references to colour in this figure legend, the reader is referred to the web version of this paper.)

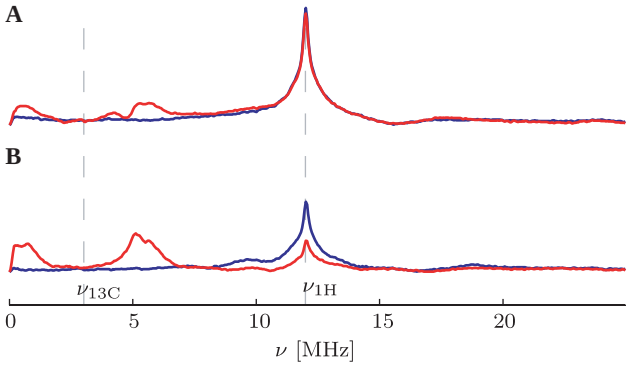

Fig. 6. τ dependence of three-pulse ESEEM spectra of $Cu(gly)_2$ (blue) and ^{13}C-labelled $Cu(gly)_2$ (red) for (A) $\tau = 180$ ns and (B) $\tau = 420$ ns. (For interpretation of the references to colour in this figure legend, the reader is referred to the web version of this paper.)

that the ^{13}C modulations have significantly dephased already during the time τ [1].

The suppression effect of the ^{13}C modulations on the ^{1}H signals is also visible. It can already be seen in the time traces in Fig.5B, where the increase of the ^{13}C modulations is accompanied by a decrease of the ^{1}H modulations. As a result, the broad ^{1}H peak in the spectra in Fig.6B is reduced by a factor of 2 in the presence of ^{13}C.

HYSCORE spectra of the two Cu(II) glycine samples were measured at 337 mT, corresponding to the absorption maximum of the EPR spectrum. As in the three-pulse ESEEM experiments, the recorded amplitudes are directly comparable without any scaling. The (+,+) quadrants of the HYSCORE spectra are depicted in Fig. 7. Lines due to strongly coupled protons (marked by arrows) are significantly reduced in amplitude in the fully ^{13}C-labelled sample. Simultaneously, a series of $^{1}H/^{13}C$ combination peaks appear. A skyline projection of the ^{1}H region onto the abscissa as shown in Fig. 8 reveals that the ^{1}H SQ/SQ peaks are reduced in amplitude by more than 50%. The amplitudes of the ^{1}H SQ and DQ matrix peaks are reduced by 35 and 45%, respectively.

An estimation of the modulation depth parameter of the observed ^{13}C nuclei from the recorded HYSCORE spectra gives $k < 0.2$. Already for such a small k, the suppression is substantial. For larger k values, e.g., from ^{14}N nuclei, the suppression effect will be even more pronounced.

5. Discussion

Although the analysis in Section 3 has been carried out for two $I = 1/2$ nuclei only, numerical simulations show that multinuclear systems with $I > 1/2$ nuclei behave in a similar way.

In systems of biological relevance, there often are one or several ^{14}N nuclei giving rise to deep modulations. As

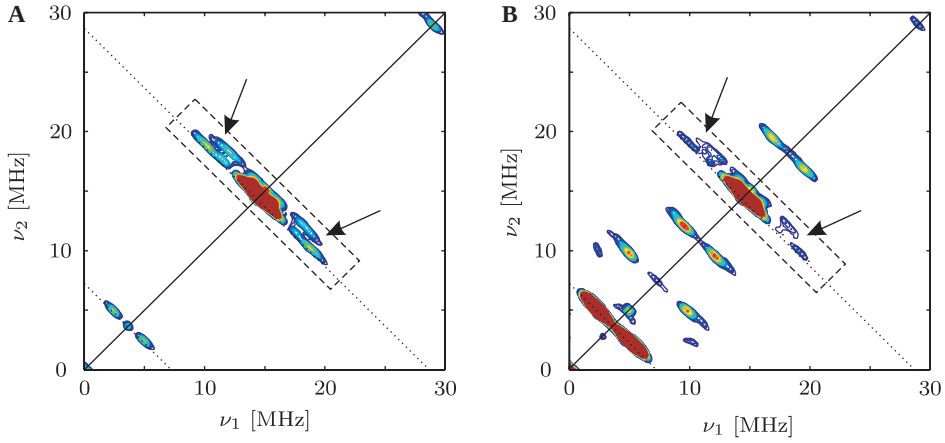

Fig. 7. HYSCORE spectra of (A) $Cu(gly)_2$ with carbon in natural abundance, (B) $Cu(gly)_2$ with ^{13}C-labelled glycine. Parameters $B_0 = 337$ mT, $\nu_{mw} = 9.770$ GHz, $\tau = 100$ ns, all pulse lengths 16 ns. The same contour levels have been used for both spectra. The ^1H SQ/SQ peaks affected by ^{13}C are marked with arrows.

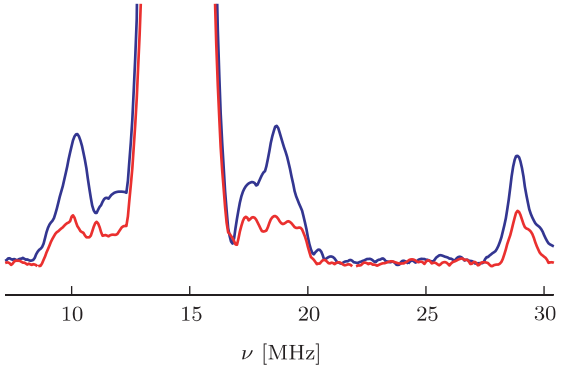

Fig. 8. Skyline projection onto the abscissa of the ^1H peak regions from the HYSCORE spectra of Fig. 7 (dashed boxes). Blue, $Cu(gly)_2$ with carbon in natural abundance; red, $Cu(gly)_2$ with ^{13}C-labelled glycine. (For interpretation of the references to colour in this figure legend, the reader is referred to the web version of this paper.)

a consequence, the ^1H signals are strongly suppressed and can fall below the noise level. Many Co(II) systems with a d_{z^2} groundstate and equatorially coordinated nitrogen nuclei exhibit this behaviour. Hence, the absence of ^1H signals in three-pulse ESEEM and HYSCORE spectra of such systems does not necessarily mean that there are no ^1H hyperfine couplings.

Care has also to be exercised when spectra of compounds in non-deuterated and deuterated solvents are compared. Such experiments are often used to identify exchangeable protons. A disappearance or reduction in intensity of certain ^1H lines helps to assign peaks to particular nuclei. However, deuterons with deep modulations can suppress ^1H peaks, which might lead to the wrong assignment of exchangeable protons.

The cross-suppression effect is inherent in the spin dynamics of standard three-pulse ESEEM and HYSCORE experiments and cannot be eliminated by any choice of experimental parameters.

However, in systems where nuclei with deep modulations and low frequencies affect ^1H signals, τ can be chosen so that the τ-dependent blind spot term b in Eq. (6) is minimal for these nuclei and maximal close to the ^1H Larmor frequency, e.g.

$$\tau = \tfrac{1}{2}|\nu_{1H}| \approx 35 \text{ ns} \tag{23}$$

for magnetic fields around 340 mT. Such a short τ value significantly dampens the ^{14}N peaks, which usually have frequencies below 5 MHz. For a nuclear frequency of 5 MHz, the τ-dependent term b is 0.250, for 2 MHz it is 0.087. The reduced amplitude of the ^{14}N peaks also reduces the cross-suppression effect on the ^1H peaks. For τ values below 100 ns the echo is formed within the dead time, and remote-echo detection [1] has to be used for both three-pulse ESEEM and HYSCORE experiments. This requires three additional pulses, which reduce the overall sensitivity of the experiment.

There are two experimental alternatives to the standard sequences which employ nuclear coherence generators different from the two-pulse generator $\pi/2$–τ–$\pi/2$ used in three-pulse ESEEM and HYSCORE.

One possibility is to use experiments with matched pulses [1]. Matched pulses can be used to enhance the modulation depth of protons compared to that of ^{14}N and similar nuclei. As with remote-echo detection, the overall sensitivity is often lower than in the standard sequences. However, it has already been successfully applied [13].

Stimulated soft ESEEM [1] could be used instead of standard three-pulse ESEEM to selectively measure modulations with frequencies within a defined region of nuclear frequencies. Interference from disturbing nuclei can virtually be avoided. In addition, soft ESEEM experiments give signals with no zero-frequency component and are free of τ-dependent blind spots. However, two locked microwave frequencies are needed to per-

form the experiment, and its viability for disordered systems has yet to be assessed.

Of course, in the case of nitrogen, an isotopic substitution of ^{14}N by ^{15}N can be used to reduce the modulation depth in many cases. The cross-suppression effect is weaker, increasing the intensity of ^{1}H-SQ signals. Such an approach will work best for nitrogen nuclei with almost isotropic hyperfine couplings. In that case, the modulation depth of ^{14}N is mostly due to state mixing caused by the nuclear quadrupole interaction, and ^{15}N will feature very shallow modulations.

6. Conclusions

We have presented an analysis of an important cross-suppression effect in ESEEM spectra of multi-nuclear spin systems, which can significantly complicate spectral analysis. Nuclei with deep modulations suppress peaks from nuclei with shallow modulations. This effect cannot be eliminated experimentally, but there are several ways to alleviate its impact: isotopic substitution, a optimal choice of τ values, and matched pulses are the most practical experimental remedies.

For numerical simulations, the inclusion of all nuclei with significant modulation depth is imperative due to the strong cross suppression. An approximation using ideal pulses and the product rule is viable for sequences employing pulse lengths of up to 16 ns, if the excitation bandwidth is properly taken into account. The effect of matrix protons on other peaks in the spectrum can be neglected.

Acknowledgment

This research has been supported by the Swiss National Science Foundation.

References

[1] A. Schweiger, G. Jeschke, Principles of Pulse Electron Paramagnetic Resonance, Oxford University Press, Oxford, 2001.
[2] Y. Deligiannakis, M. Louloudi, N. Hadjiliadis, Electron spin echo envelope modulation (ESEEM) spectroscopy as a tool to investigate the coordination environment of metal centers, Coord. Chem. Rev. 204 (2000) 1–112.
[3] E. Reijerse, S.A. Dikanov, Electron spin echo envelope modulation spectroscopy on orientationally disordered systems: line shape singularities in $S = 1/2$, $I = 1/2$ spin systems, J. Chem. Phys. 95 (1991) 836–845.
[4] S.A. Dikanov, M.K. Bowman, Cross-peak lineshape of two-dimensional ESEEM spectra in disordered $S = 1/2$, $I = 1/2$ spin systems, J. Magn. Reson. A 116 (1995) 125–128.
[5] A.V. Astashkin, A.M. Raitsimring, Properties of the HYSCORE spin echo signal, J. Magn. Reson. 148 (2001) 379–387.
[6] S.A. Dikanov, A.M. Tyryshkin, M.K. Bowman, Intensity of cross-peaks in Hyscore spectra of $S = 1/2$, $I = 1/2$ spin systems, J. Magn. Reson. 144 (2000) 228–242.
[7] S.A. Dikanov, A.A. Shubin, V.N. Parmon, Modulation effects in the electron spin echo resulting from hyperfine interaction with a nucleus of an arbitrary spin, J. Magn. Reson. 42 (1981) 474–487.
[8] W.B. Mims, Envelope modulation in spin-echo experiments, Phys. Rev. B 5 (1972) 2409–2419.
[9] A.M. Tyryshkin, S.A. Dikanov, D. Goldfarb, Sum combination harmonics in four-pulse ESEEM spectra. Study of the ligand geometry in aqua–vanadyl complexes in polycrystalline and glass matrices, J. Magn. Reson. A 105 (1993) 271–283.
[10] J. Harmer, S. Van Doorlaer, I. Gromov, A. Schweiger, Corrin nitrogens and remote dimethylbenzimidazole nitrogen interactions in Cob(II)alamin studied with HYSCORE at X- and Q-band, Chem. Phys. Lett. 358 (2002) 8–16.
[11] L. Liesum, A. Schweiger, Multiple quantum coherence in HYSCORE spectra, J. Chem. Phys. 114 (2001) 9478–9488.
[12] H.-J. Scholl, J. Hüttermann, ESR and ENDOR of Cu(II) complexes with nitrogen donors: probing parameters for prosthetic group modeling of superoxide dismutase, J. Phys. Chem. 92 (1992) 9684–9691.
[13] E. Vinck, S. Van Doorslaer, Analysing low-spin ferric complexes using pulse EPR techniques: a structure determination of bis (4-methylimidazole) (tetraphenylporphyrinato)iron(III), Phys. Chem. Chem. Phys. 6 (2004) 5324–5330.